

Entanglement generation and transfer between remote atomic qubits interacting with squeezed field

Paulo José dos Reis* and S. Shelly Sharma†

Departamento de Física, Universidade Estadual de Londrina, Londrina 86051-990, PR Brazil

N. K. Sharma‡

Departamento de Matemática, Universidade Estadual de Londrina, Londrina 86051-990 PR, Brazil

A pair of two level atoms A_1A_2 , prepared either in a separable state or in an entangled state, interacts with a single mode of two mode squeezed cavity field while a third atomic qubit B interacts with the second mode of the squeezed field in a remote cavity. We analyze, numerically, the generation, sudden death and revival of three qubit entanglement as a function of initial entanglement of qubits A_1A_2 and degree of squeezing of electromagnetic field. Global negativity of partially transposed state operator is used to quantify the entanglement of three atom state. It is found that the initial entanglement of two mode field as well as that of the pair A_1A_2 , both, contribute to three atom entanglement. A maximally entangled single excitation Bell pair in first cavity and two mode field with squeeze parameter $s = 0.64$ are the initial conditions that optimize the peak value of three qubit mixed state entanglement. A smaller value of $s = 0.4$ under similar conditions is found to generate a three qubit mixed state with comparable entanglement dynamics free from entanglement sudden death.

I. INTRODUCTION

Quantum entanglement is an essential physical resource in communication protocols [1] and information processing [2]. Remote quantum systems may become entangled through interaction with a third quantum system as in cavity QED experiments [3], where entanglement of photon state in two cavities results from interaction with an atomic qubit. On the other hand, atomic qubits having shared quantized motion may be entangled through interaction with electromagnetic field as in ion traps [4]. A parametric down converter is known to generate two mode electromagnetic field in a squeezed state with the entanglement of two modes determined by squeeze parameter. Direct observation of 10 dB squeezing of quantum noise of light, has been reported recently [5]. As such, two mode squeezed states are a potential entanglement resource. It has been shown that the field state entanglement can be transferred to a pair of remote atoms [6, 7] or three remote atoms [8] distributed in two isolated cavities. Paternostro et al., [9] have investigated the connection between entanglement-transfer to a pair of non-interacting two-level systems and statistical properties of entangled two-mode continuous variable resource. State engineering through bilinear interactions between two remote qubits and two-mode Gaussian light fields has, also, been reported [10]. An interesting study of entanglement transfer from a three-mode quantized field to a system of three spatially separated qubits, each one made of a two-level atom resonantly coupled to a cavity mode has been presented in ref. [11]. Entanglement transfer from freely propagating quantized light to an atomic system has been achieved experimentally [12–14]. In this article, distributed tripartite entanglement generation through entanglement transfer from two mode squeezed field to three atomic qubits in two cavities, is proposed. Two level atoms, A_1 and A_2 , prepared either in a separable state or in an entangled state interact with a single mode of two mode squeezed field in a cavity held by Alice, while a third atom B located in a remote cavity interacts with the second mode of the squeezed field. We analyze, analytically and numerically, the entanglement dynamics of atomic qubits after tracing over the field degrees of freedom. This is a natural way of obtaining a distributed channel for quantum communication, when the entangled resource is the continuous variable (CV) state of a photonic system.

Global negativity [15–17] and K -way negativities [19] are used to qualify and quantify the free entanglement of three qubit mixed state. In our earlier article [8], the three atom system in separable initial state was found to develop W -like entanglement exhibiting entanglement sudden death (ESD) and entanglement sudden revival (ESR). Entanglement sudden death, reported by Yu and Eberly [20, 21] for the first time, refers to disappearance of entanglement in finite time. ESD observed experimentally for entangled photon pairs [22], and atomic ensembles [23]

*Electronic address: paulojreis@uel.br

†Electronic address: shelly@uel.br

‡Electronic address: nsharma@uel.br

is a hindrance to using the system for implementing useful protocols. It is known that entanglement can be distilled from a three qubit pure or mixed state having free entanglement. With this in mind, we look for initial conditions on three atom state and squeezed field state so as to reduce the time interval between ESD and ESR or make the phenomenon disappear altogether. The three qubit entanglement generation, sudden death and revival dynamics depends strongly on degree of squeezing of two mode vacuum state and initial entanglement of pair $A_1 A_2$. It is found that the initial state quantum correlations of qubits $A_1 A_2$ translate into an increase in remote qubit entanglement and a remarkable change in the rate at which the entanglement decays.

The paper is organized as follows. A brief description of the model and procedure to obtain analytical expressions for three atom state at current time from different initial states of atoms and field are given in Section II. Section III focuses on a comparative analysis of remote qubit entanglement dynamics for different initial states. A summary of results is presented in section IV.

II. THE MODEL

We consider the entanglement transfer process from a two-mode squeezed vacuum field to a system of three localized and spatially distributed qubits. An entangled two-mode CV state is generated with an off-line process. Two atomic qubits, A_1 and A_2 , localized inside a single mode cavity c_1 interact resonantly with one mode of the field. A third two level atom B , located in cavity c_2 , interacts with the second field mode. We assume that each mode of the squeezed field is first injected into a cavity and then interacts resonantly with atomic qubits. The scheme used is analogous to that of our earlier work in which all three atomic qubits are prepared, initially, in their ground states. Here we generalize the model to investigate the effect of initial two qubit entanglement on tripartite entanglement generation. A search for squeeze parameter value and initial two qubit entangled state, suitable for generating three qubit correlations that overcome entanglement sudden death, is carried out. The action of two-mode squeezing operator

$$\hat{S}(s) = \exp(-s\hat{a}\hat{b} + s\hat{a}^\dagger\hat{b}^\dagger), \quad (1)$$

on two-mode vacuum state $|0, 0\rangle$ generates two-mode squeezed vacuum state

$$|\Psi_F\rangle = \frac{1}{\cosh s} \sum_{n=0}^{\infty} (\tanh s)^n |n, n\rangle, \quad (2)$$

where \hat{a}^\dagger , \hat{a} and \hat{b}^\dagger , \hat{b} are the bosonic creation and annihilation operators for modes one and two, respectively. The two mode squeezed state is an entangled state having bipartite entanglement determined by value of squeeze parameter s . The variances of quadrature operators for $|\Psi_F\rangle$ are below the vacuum limit. Simple linear coupling is used to inject one of the field modes from a two mode field source into cavity c_1 in vacuum state, while the second field mode is directed to the remote cavity c_2 in vacuum state. Neglecting cavity mode dissipation, the resonant cavity-CV field mode coupling is described by beam splitter operator

$$\hat{B}_i(\theta) = \exp \left[-\frac{\theta}{2} (\hat{f}_i^\dagger \hat{c}_i - \hat{f}_i \hat{c}_i^\dagger) \right], \quad i = 1, 2, \quad (3)$$

where \hat{c}_i (\hat{f}_i) and \hat{c}_i^\dagger (\hat{f}_i^\dagger) are creation and annihilation operators for photons inside the i^{th} cavity (external field), respectively. The coupling between the cavity field and the external field is determined by the cavity mirror transmittance coefficient $T(\theta) = \cos^2(\frac{\theta}{2})$. After injecting the two-mode non-classical field into independent cavities c_1 and c_2 , the cavity field at $t = 0$ is found to be in a mixed state

$$\hat{\rho}_F(0) = \left(\frac{1}{\cosh s} \right)^2 \sum_{n,m=0}^{\infty} \sum_{k,l=0}^{\min[n,m]} (\tanh s)^{n+m} G_{kl}^{nm}(\theta) \quad (4)$$

$$\times (|n-k\rangle_{c_1} \langle m-k|) (|n-l\rangle_{c_2} \langle m-l|), \quad (5)$$

where

$$G_{kl}^{nm}(\theta) = C_k^n(\theta) C_k^m(\theta) C_l^n(\theta) C_l^m(\theta), \quad (6)$$

and

$$C_k^n(\theta) = \sqrt{\frac{n!}{k!(n-k)!}} \cos^k \frac{\theta}{2} \sin^{n-k} \frac{\theta}{2}. \quad (7)$$

The degree of entanglement of $\hat{\rho}_F(0)$ is determined by the transmittance coefficient $T(\theta)$ and is maximal at $T(\theta) = 1$. The beam splitter has a disentangling effect. The composite field $\hat{\rho}_F(0)$ is in a mixed state for $\cos \theta < 1$, while when $\cos \theta = \sin \theta$ it is in a separable state.

A. Atom Field Interaction

Consider N identical two level atoms interacting via dipole coupling with a single-mode quantized radiation field in a resonator. The ground and excited states for the atom i ($i = 1$ to N) are, respectively, denoted by $|g\rangle_i$ and $|e\rangle_i$. Spin operators for i^{th} atomic qubit are defined as $\hat{\sigma}_z^i = |e\rangle_i \langle e| - |g\rangle_i \langle g|$, $\hat{\sigma}_-^i = |g\rangle_i \langle e|$ and $\hat{\sigma}_+^i = |e\rangle_i \langle g|$. Defining collective spin variables of N two-level atoms as $\hat{\sigma}_k = \sum_{i=1,N} \hat{\sigma}_k^i$ where $k = (z, +, -)$, we may construct the eigenbasis of operators $\hat{\sigma}^2$ and $\hat{\sigma}_z$ to represent N atom internal states. A typical basis vector in coupled basis is written as $|\sigma, m_\sigma\rangle$, with eigen values of $\hat{\sigma}^2$ and $\hat{\sigma}_z$ given by $\sigma(\sigma + 2)$ and m_σ , respectively.

In the absence of atom-field coupling, the free Hamiltonian given by $\hat{H}_{at} = \frac{\hbar\omega_a}{2}\hat{\sigma}_z$ for atomic qubits and $\hat{H}_{cav} = \hbar\omega_0(\hat{a}^\dagger\hat{a})$ for cavity field, determines the system dynamics. Here $\hbar\omega_a$ is the level splitting of the two-level atoms, ω_0 is a frequency of the electromagnetic field and $\hat{a}^\dagger(\hat{a})$ is photon creation (annihilation) operator. The atom-field interaction Hamiltonian given by Tavis Cummings model (TCM) [24] in interaction picture and rotating wave approximation, has the form

$$\hat{H}_{int} = \hbar g_c \sum_{i=1,N} (\hat{a}\hat{\sigma}_+^i + \hat{a}^\dagger\hat{\sigma}_-^i), \quad (8)$$

for resonant ($\omega_0 = \omega_a$) interaction of dipoles with cavity field. Here g_c is the atom-field coupling strength assumed to be the same for all atoms. Since the Hamiltonian commutes with $(\hat{\sigma})^2$, the unitary evolution operator $\hat{U}_1(\tau) = \exp\left[\frac{-i}{\hbar}\hat{H}t\right]$ conserves the quantum number σ .

For two atoms the coupled basis vectors are the set of symmetric states $|2, -2\rangle$, $|2, 0\rangle$, $|2, 2\rangle$ and antisymmetric state $|0, 0\rangle$. The number state of cavity field is represented by $|n\rangle$. For two atoms in cavity c_1 , interacting resonantly ($\omega_0 - \omega_a = \delta = 0$) with n photons, interaction hamiltonaia is represented by matrix

$$H_{int} = \begin{bmatrix} \hbar\omega_0 n & \hbar g\sqrt{2n} & 0 \\ \hbar g\sqrt{2n} & \hbar\omega_0 n & \hbar g\sqrt{2(n-1)} \\ 0 & \hbar g\sqrt{2(n-1)} & \hbar\omega_0 n \end{bmatrix},$$

in the basis $|2, -2, n\rangle$, $|2, 0, n-1\rangle$, and $|2, 2, n-2\rangle$. Using eigenvalues and eigenbasis of H_{int} , the unitary operator that governs the evolution of two atoms in cavity c_1 is found to be

$$U_1^n(\tau) = \exp^{-i\omega_0 n \tau} \begin{pmatrix} \frac{B_n^2 \cos(f_n \tau) + A_n^2}{A_n^2 + B_n^2} & \frac{-iB_n \sin(f_n \tau)}{\sqrt{(A_n^2 + B_n^2)}} & \frac{A_n B_n [\cos(f_n \tau) - 1]}{A_n^2 + B_n^2} \\ \frac{-iB_n \sin(f_n \tau)}{\sqrt{(A_n^2 + B_n^2)}} & \cos(f_n \tau) & \frac{-iA_n \sin(f_n \tau)}{\sqrt{(A_n^2 + B_n^2)}} \\ \frac{A_n B_n [\cos(f_n \tau) - 1]}{A_n^2 + B_n^2} & \frac{-iA_n \sin(f_n \tau)}{\sqrt{(A_n^2 + B_n^2)}} & \frac{[A_n^2 \cos(f_n \tau) + B_n^2]}{A_n^2 + B_n^2} \end{pmatrix}, \quad (9)$$

where interaction parameter $\tau = gt$, $f_n = \sqrt{2(2n-1)}$, $A_n = \sqrt{2(n-1)}$, and $B_n = \sqrt{2n}$. For a single atom the basis states $|1, -1\rangle$ ($|1, 1\rangle$) stands for the ground (excited) state of the atom. The unitary matrix that determines the state evolution due to interaction of a single atom with field in cavity c_2 , reads as

$$U_2^m(\tau) = \begin{pmatrix} \cos(\sqrt{m}\tau) & -i \sin(\sqrt{m}\tau) \\ -i \sin(\sqrt{m}\tau) & \cos(\sqrt{m}\tau) \end{pmatrix}, \quad (10)$$

in the basis $|1, -1, m\rangle, |1, 1, m-1\rangle$. The evolution operator for the two cavity composite system is obtained by taking the tensor product that is

$$U_{12}^{nm}(\tau) = U_1^n(\tau) \otimes U_2^m(\tau). \quad (11)$$

For a given atomic initial state

$$\hat{\rho}_{A_1 A_2 B}(0) = |\Phi\rangle \langle \Phi| = (|\Phi_{A_1 A_2}(0)\rangle \langle \Phi_{A_1 A_2}(0)|)_{c_1} (|\Phi_B(0)\rangle \langle \Phi_B(0)|)_{c_2} \quad (12)$$

and field state $\hat{\rho}_F(0)$ (Eq. (4)), using unitary operators of Eqs. (9) and (10), state of composite system after interaction time $t = \tau/g_c$ reads as

$$\begin{aligned} \hat{\rho}(\tau) &= \hat{U}_1(\tau) \otimes \hat{U}_2(\tau) \hat{\rho}_{A_1 A_2 B}(0) \otimes \hat{\rho}_F(0) \hat{U}_1^\dagger(\tau) \otimes \hat{U}_2^\dagger(\tau) \\ &= \left(\frac{1}{\cosh s} \right)^2 \sum_{n,m=0}^{\infty} \sum_{k,l=0}^{\min[n,m]} (\tanh s)^{n+m} G_{kl}^{nm}(\theta) \left| \Phi_{A_1 A_2 B}^{n-k,n-l}(\tau) \right\rangle \left\langle \Phi_{A_1 A_2 B}^{m-k,m-l}(\tau) \right|, \end{aligned} \quad (13)$$

where

$$\left| \Phi_{A_1 A_2 B}^{n-k,n-l}(\tau) \right\rangle = \hat{U}_{12}^{n-k,n-l}(\tau) |\Phi_{A_1 A_2}(0), n-k\rangle_{c_1} |\Phi_B(0), n-l\rangle_{c_2}. \quad (14)$$

The information about the effective evolution of three atom entanglement is contained in the state operator $\hat{\rho}_{A_1 A_2 B}(\tau)$, obtained from $\hat{\rho}(\tau)$ upon partial trace over the CV degrees of freedom that is

$$\hat{\rho}_{A_1 A_2 B}(\tau) = Tr_F(\hat{\rho}(\tau)). \quad (15)$$

The matrix $\hat{\rho}_{A_1 A_2 B}(\tau)$ is used to analyze, numerically, the entanglement generation between the remote qubit B and the pair of qubits $A_1 A_2$.

B. Atoms in Initial State $|\Phi_1^\alpha(0)\rangle = \sqrt{\alpha}|000\rangle + \sqrt{(1-\alpha)}|110\rangle$

We consider two different types of atomic initial states. Firstly, two atoms in cavity c_1 are prepared in state

$$|\Phi_{A_1 A_2}^\alpha(0)\rangle = \sqrt{\alpha}|2, -2\rangle + \sqrt{(1-\alpha)}|2, 2\rangle, \quad (16)$$

while the atom in cavity c_2 is in ground state at $t = 0$. The two atoms have varying degree of entanglement for $0 < \alpha < 1$. States $|\Phi_{A_1 A_2}^0(0)\rangle$ and $|\Phi_{A_1 A_2}^1(0)\rangle$ are separable states. Interaction of atoms with two mode squeezed field is known to generate entanglement of qubit B with pair $A_1 A_2$ [8], however, the role of initial entanglement of atoms in entanglement generation is not known. Our object is to investigate if initial entanglement of atoms serves as a catalyst in the process of entanglement transfer or hinders it. The maximal value of entanglement generated and inhibition of zero entanglement zones are considered as the pointers or indicators of such effects.

Associating computational basis state $|0\rangle$ to atomic ground state and $|1\rangle$ to an atom in excited state, the initial three atom state is

$$\begin{aligned} |\Phi_1^\alpha(0)\rangle &= |\Phi_{A_1 A_2}^\alpha(0)\rangle |\Phi_B(0)\rangle = \sqrt{\alpha}|000\rangle + \sqrt{(1-\alpha)}|110\rangle, \\ \hat{\rho}_A^\alpha(0) &= |\Phi_1^\alpha(0)\rangle \langle \Phi_1^\alpha(0)|. \end{aligned}$$

The state of atom-field composite system after interaction time t , obtained by using Eq. (13), reads as

$$\hat{\rho}^\alpha(\tau) = \left(\frac{1}{\cosh s} \right)^2 \sum_{n,m=0}^{\infty} \sum_{k,l=0}^{\min[n,m]} (\tanh s)^{n+m} G_{kl}^{nm}(\theta) \left| \Phi_{A_1 A_2 B}^{n-k,n-l}(\tau) \right\rangle_\alpha \left\langle \Phi_{A_1 A_2 B}^{m-k,m-l}(\tau) \right|. \quad (17)$$

Exact analytic expression for $\left| \Phi_{A_1 A_2 B}^{n-k,n-l}(\tau) \right\rangle_\alpha$ is given in Appendix (IV). The state operator for atomic qubits A_1 , A_2 , and B is obtained from $\hat{\rho}^\alpha(\tau)$ by tracing out the field modes that is

$$\hat{\rho}_A^\alpha(\tau) = Tr_F(\hat{\rho}^\alpha(\tau)). \quad (18)$$

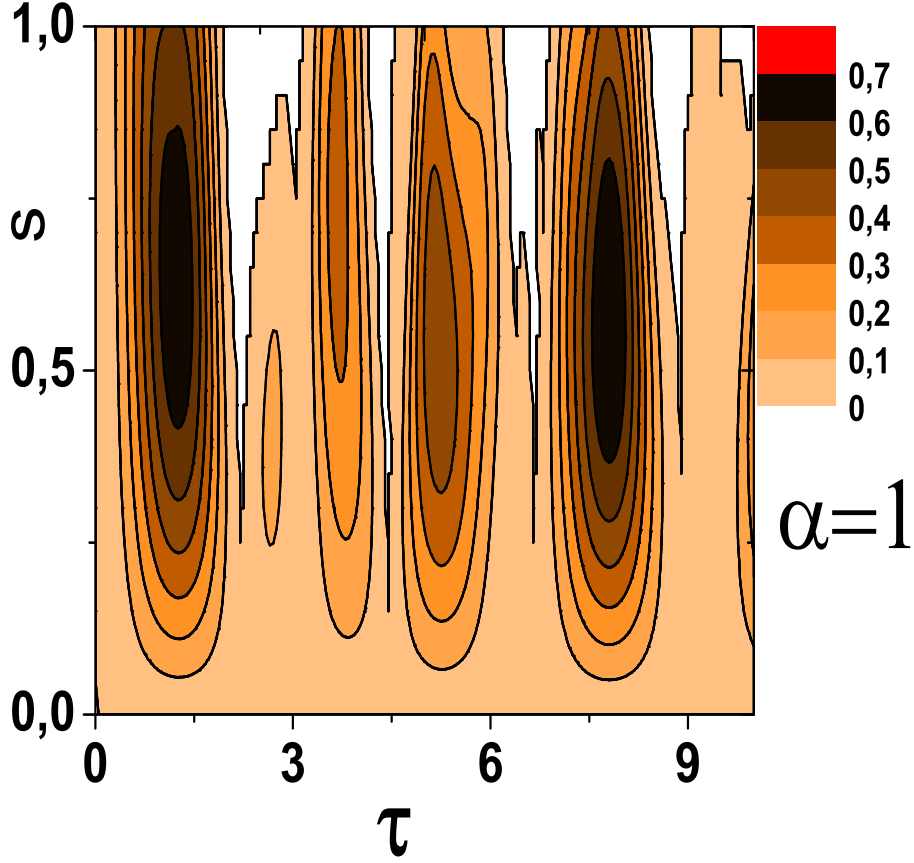


FIG. 1: Contour plot of global negativity $N_G^B(\rho_A^{\alpha=1}(\tau))$ as a function of s and τ . Area in white represents zero negativity.

The matrix $\rho_A^\alpha(\tau)$ in the basis $|2, -2\rangle_1 |1, -1\rangle_2, |2, 0\rangle_1 |1, -1\rangle_2, |2, 2\rangle_1 |1, -1\rangle_2, |2, -2\rangle_1 |1, 1\rangle_2, |2, 0\rangle_1 |1, 1\rangle_2, |2, 2\rangle_1 |1, 1\rangle_2$, has the form

$$\rho_A^\alpha(\tau) = \begin{pmatrix} (\rho_A^\alpha(\tau))_{11} & 0 & (\rho_A^\alpha(\tau))_{13} & 0 & (\rho_A^\alpha(\tau))_{15} & 0 \\ 0 & (\rho_A^\alpha(\tau))_{22} & 0 & (\rho_A^\alpha(\tau))_{42} & 0 & (\rho_A^\alpha(\tau))_{26} \\ (\rho_A^\alpha(\tau))_{13} & 0 & (\rho_A^\alpha(\tau))_{33} & 0 & (\rho_A^\alpha(\tau))_{53} & 0 \\ 0 & (\rho_A^\alpha(\tau))_{42} & 0 & (\rho_A^\alpha(\tau))_{44} & 0 & (\rho_A^\alpha(\tau))_{46} \\ (\rho_A^\alpha(\tau))_{15} & 0 & (\rho_A^\alpha(\tau))_{53} & 0 & (\rho_A^\alpha(\tau))_{55} & 0 \\ 0 & (\rho_A^\alpha(\tau))_{26} & 0 & (\rho_A^\alpha(\tau))_{46} & 0 & (\rho_A^\alpha(\tau))_{66} \end{pmatrix}. \quad (19)$$

C. Atoms in Initial State $|\Phi_2(0)\rangle = \frac{1}{\sqrt{2}}(|010\rangle + |100\rangle)$

Another possibility, where pair of qubits A_1 and A_2 are in an entangled state at $t = 0$ arises with the atoms prepared initially in states $|\Phi_{A_1 A_2}(0)\rangle = |2, 0\rangle$, and $|\Phi_B(0)\rangle = |1, -1\rangle$, that is

$$|\Phi_2(0)\rangle = \frac{1}{\sqrt{2}}(|010\rangle + |100\rangle), \quad \hat{\rho}_A^I(0) = |\Phi_2(0)\rangle \langle \Phi_2(0)|.$$

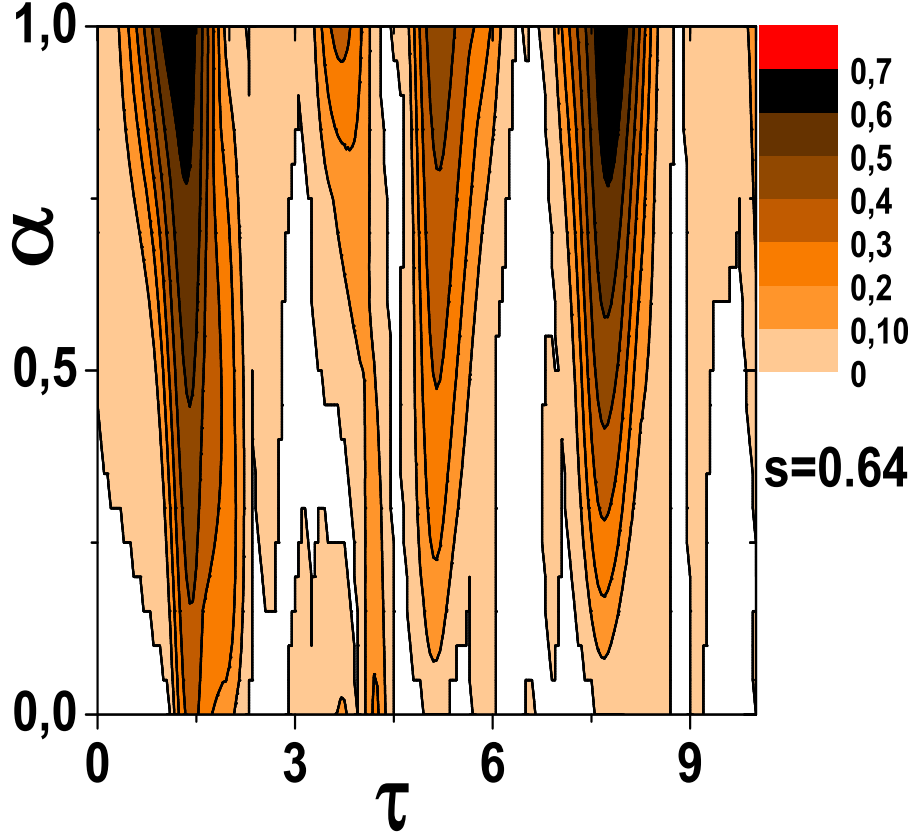


FIG. 2: Contour plot of global negativity $N_G^B(\rho_A^\alpha(\tau))$ versus α and τ for $s = 0.64$.

Using Eq. (13), the state of composite system after interaction time t is found to be

$$\begin{aligned}\hat{\rho}_A^{II}(\tau) &= \hat{U}_{12}(\tau)\hat{\rho}_A^{II}(0) \otimes \hat{\rho}_F(0)\hat{U}_{12}^\dagger(\tau) \\ &= \left(\frac{1}{\cosh s}\right)^2 \sum_{n,m=0}^{\infty} \sum_{k,l=0}^{\min[n,m]} (\tanh s)^{n+m} G_{kl}^{mm}(\theta) \left| \Phi_{A_1 A_2 B}^{n-k,n-l}(\tau) \right\rangle \left\langle \Phi_{A_1 A_2 B}^{m-k,m-l}(\tau) \right|,\end{aligned}\quad (20)$$

with $\left| \Phi_{A_1 A_2 B}^{n-k,n-l}(\tau) \right\rangle$ as listed in Appendix (IV). The corresponding atomic density operator $\hat{\rho}_A^{II}(\tau)$, in the basis $|2, -2\rangle_{c_1} |1, -1\rangle_{c_2}, |2, 0\rangle_{c_1} |1, -1\rangle_{c_2}, |2, 2\rangle_{c_1} |1, -1\rangle_{c_2}, |2, -2\rangle_{c_1} |1, 1\rangle_{c_2}, |2, 0\rangle_{c_1} |1, 1\rangle_{c_2}, |2, 2\rangle_{c_1} |1, 1\rangle_{c_2}$, reads as

$$\rho_A^{II}(\tau) = \begin{pmatrix} (\rho_A^{II}(\tau))_{11} & 0 & 0 & 0 & (\rho_A^{II}(\tau))_{15} & 0 \\ 0 & (\rho_A^{II}(\tau))_{22} & 0 & 0 & 0 & (\rho_A^{II}(\tau))_{26} \\ 0 & 0 & (\rho_A^{II}(\tau))_{33} & 0 & 0 & 0 \\ 0 & 0 & 0 & (\rho_A^{II}(\tau))_{44} & 0 & 0 \\ (\rho_A^{II}(\tau))_{15} & 0 & 0 & 0 & (\rho_A^{II}(\tau))_{55} & 0 \\ 0 & (\rho_A^{II}(\tau))_{26} & 0 & 0 & 0 & (\rho_A^{II}(\tau))_{66} \end{pmatrix}. \quad (21)$$

III. THREE QUBIT ENTANGLEMENT DYNAMICS

In our earlier article [8], the three atom system in separable initial state was found to develop W -like entanglement exhibiting entanglement sudden death (ESD) and revival (ESR). Entanglement sudden death refers to disappearance

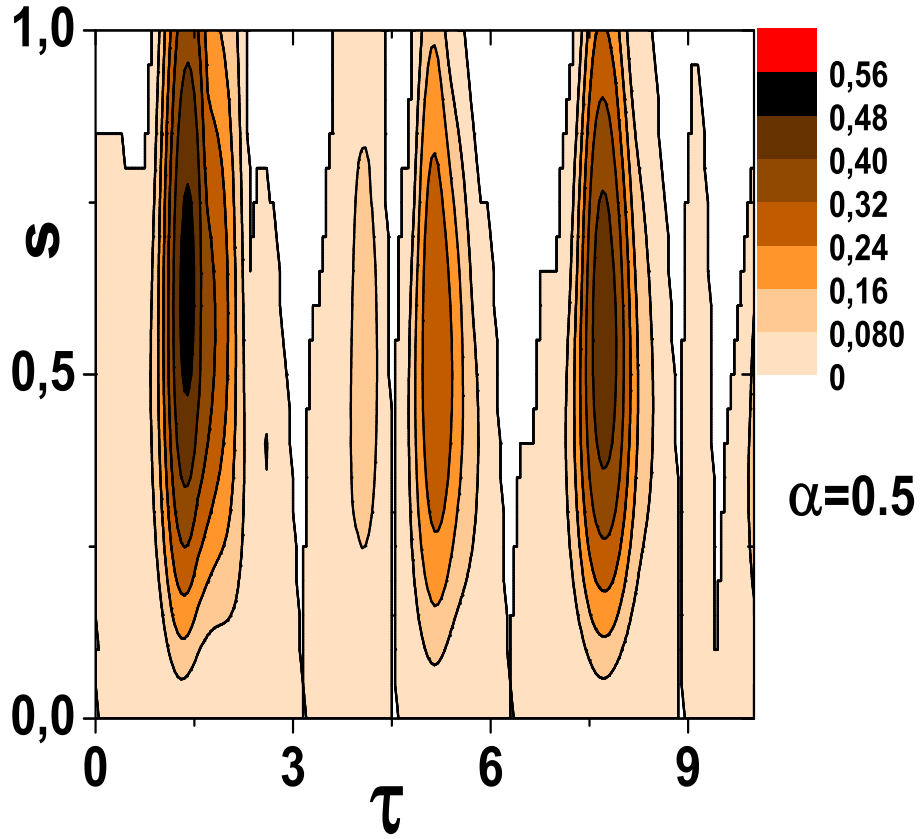


FIG. 3: Contour plot of global negativity $N_G^B(\rho_A^{\alpha=0.5}(\tau))$ as a function of s and τ .

of entanglement of the state in finite time and was reported by Yu and Eberly [20, 21] for the first time. ESD has been observed experimentally for entangled photon pairs [22], and atomic ensembles [23]. It is a hindrance to using the system for implementing useful protocols. We analyze, numerically, the dependence of three qubit entanglement generation on the degree of squeezing of electromagnetic field and initial state entanglement of qubits A_1 and A_2 . Since the focus is on the effect of initial state entanglement of qubits in cavity c_1 on entanglement transfer from CV field and generation of tripartite distributed entanglement, for simplicity, we neglect the effect of the mirror transmittance, i.e., consider $T(\theta) = 1$. For appropriate choice of squeeze parameter the time interval between ESD and ESR (Entanglement sudden revival) is found to become shorter or disappear altogether.

A. Entanglement of qubit B with pair $A_1 A_2$

Fortran codes were written to calculate, numerically, the system dynamics for initial states with varying degree of field state entanglement and two atom entanglement in cavity c_2 , using analytic expressions obtained in section II. To analyze the entanglement of remote qubit B in cavity c_2 with qubits $A_1 A_2$ in cavity c_1 , the global negativity of partially transposed state operator was calculated. Writing a general three qubit as

$$\hat{\rho} = \sum_{\substack{i_1 i_2 i_3 \\ j_1 j_2 j_3}} \langle i_1 i_2 i_3 | \hat{\rho} | j_1 j_2 j_3 \rangle | i_1 i_2 i_3 \rangle \langle j_1 j_2 j_3 |, \quad (22)$$

where $|i_1 i_2 i_3\rangle$ are the basis vectors spanning 2^3 dimensional Hilbert space, the global partial transpose with respect to qubit B is constructed from the matrix elements of $\hat{\rho}$ through

$$\langle i_1 i_2 i_3 | \hat{\rho}_G^{T_B} | j_1 j_2 j_3 \rangle = \langle i_1 i_2 j_3 | \hat{\rho} | j_1 j_2 i_3 \rangle. \quad (23)$$

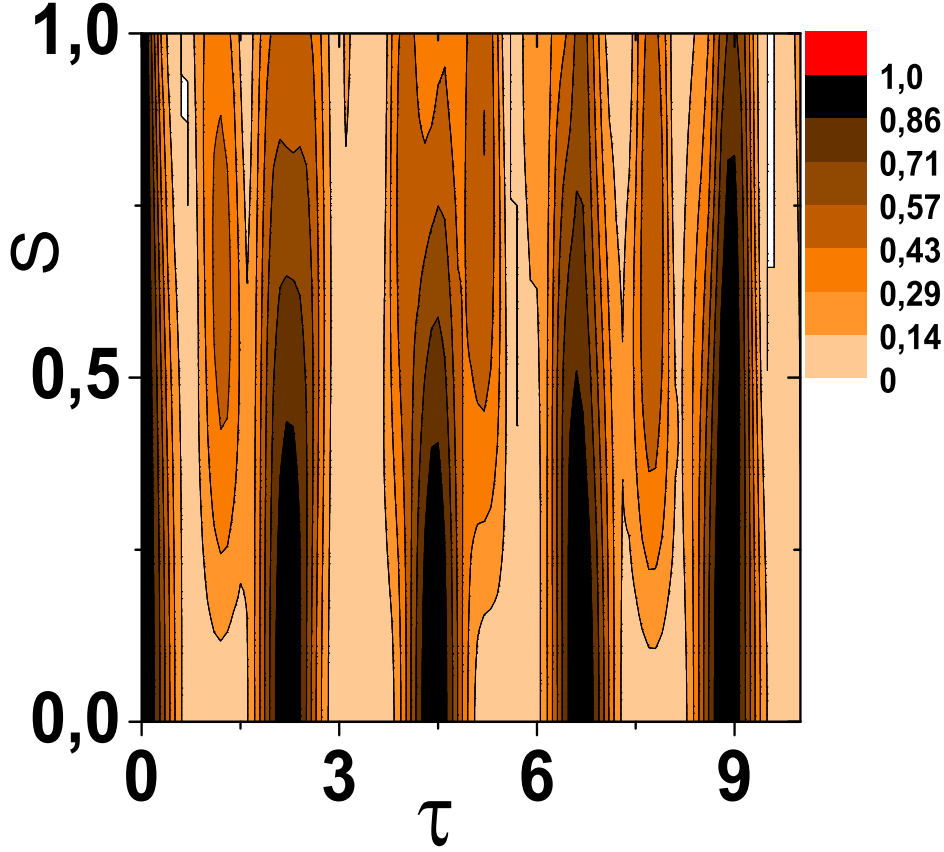


FIG. 4: Contour plot of global negativity $N_G^{A1}(\rho^{II}(\tau))$ as a function of s and τ .

The state of qubit at location A_m is labelled by $i_m = 0$ and 1 , where $m = 1, 2$. The state of qubit B is labelled by $i_3 = 0, 1$. Global negativity is defined as

$$N_G^{A_p} = \left(\|\hat{\rho}_G^{T_{A_p}}\|_1 - 1 \right), \quad (24)$$

where $\|\hat{\rho}\|_1$ is the trace norm of $\hat{\rho}$. Global negativity lies in the range 0 for a separable state to 1 for a maximally entangled state. The negativity [15–17] of $\hat{\rho}_G^{T_B}$, based on Peres-Horodecki criterion [25, 26] is a natural entanglement measure and has been shown to be an entanglement monotone [17]. As the qubits A_1 and A_2 are always in a symmetric initial state, the entanglement of qubit B with either of the qubits is the same. Therefore a negative partial transpose of $\hat{\rho}_A(\tau)$ with respect to qubit B indicates tripartite entanglement. A three qubit state may have GHZ-like or W-like tripartite [18] entanglement. In ref [19] it has been shown that a global partial transpose may be written in terms of a two way partial transpose, a three-way partial transpose and the state operator. We notice that for states $\hat{\rho}_A^\alpha(\tau)$ and $\hat{\rho}_A^{II}(\tau)$ partial transposition involves, only, matrix elements $\langle i_1 i_2 j_3 | \hat{\rho}_A(\tau) | j_1 j_2 i_3 \rangle$ with $K = \sum_{i,j=1,i < j}^3 (1 - \delta_{i,j}) = 2$. In

other words the global partial transpose $(\rho_A(\tau))_G^{T_B}$ is equal to two way partial transpose $(\rho_A(\tau))_2^{T_B}$ [19]. Therefore the entanglement of mixed state is similar to W-like entanglement of three qubit pure states. It is a natural consequence of the fact that no direct three atom interaction takes place.

Firstly, we discuss the numerical results of global negativity of partial transpose of matrix $\rho_A^\alpha(\tau)$ with respect to remote qubit B . Fig. (1) is a contour plot of $N_G^B(\rho_A^{\alpha=1}(\tau))$ as a function of squeeze parameter s and interaction parameter τ , for two atoms in separable state $|\Phi_1^{\alpha=1.0}(0)\rangle$. Entanglement of remote qubit at peak value is found to increase with s , being optimum for $s = 0.64$, where peak value of $N_G^B(\rho_a^\alpha(\tau))$ is around 0.7. However, for a fixed value of s the regions with continuously zero negativity (white) alternate with regions having finite global negativity and

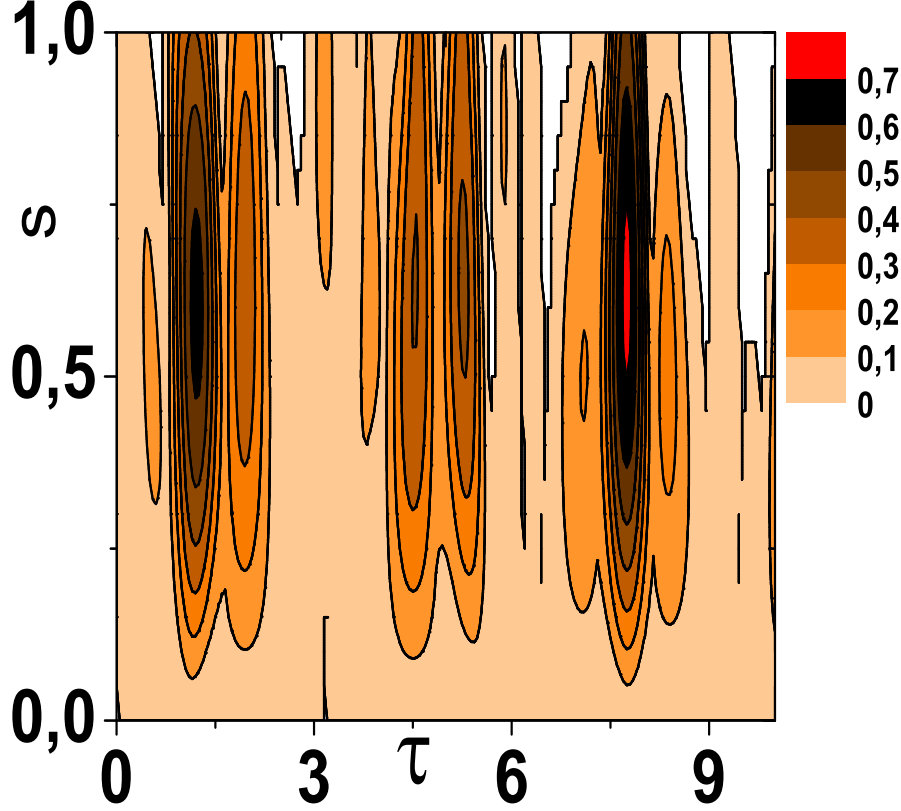


FIG. 5: Contour plot of global negativity $N_G^B(\rho_A^{II}(\tau))$ as a function of s and τ .

the meeting points represent values of τ for which entanglement sudden death or revival of entanglement occurs. A contour plot of $N_G^B(\rho_A^\alpha(\tau))$ as a function of α , τ and $s = 0.64$ displayed in Fig. (2) reveals that for $\alpha < 1$ that is an entangled state $|\Phi_{A_1 A_2}^\alpha(0)\rangle$, the global negativity strongly depends on value of α . The peak value of $N_G^B(\rho_A^\alpha(\tau))$ is found to decrease as $\alpha \rightarrow 0$ and regions with zero entanglement become wider in comparison with that for $\alpha = 1$. A comparison of linear entropy of $\rho_A^{\alpha=1}(\tau)$ and $\rho_A^{\alpha \neq 1}(\tau)$ at peak value of $N_G^B(\rho_A^\alpha(\tau))$ shows a larger value for $\rho_A^{\alpha \neq 1}(\tau)$, indicating that initial entanglement generates a noisier three qubit state than the state $\rho_A^{\alpha=1}(\tau)$.

Figure 3 displays the negativity $N_G^B(\rho_A^{\alpha=0.5}(\tau))$, versus compression parameter s and interaction parameter τ , for the initial state $|\Phi_1^{\alpha=0.5}(0)\rangle$. In this case maximum value of $N_G^B(\rho_A^{\alpha=0.5}(\tau)) = 0.5$ corresponds to $s = 0.64$ and occurs at $\tau = 7.75$. The interaction time after which entanglement dies is $\tau = 2.45$, for $s = 0.64$. When we use a compression parameter smaller than 0.64 zero negativity regions shrink pointing to a decrease in noise however the peak value of negativity tends to zero as well.

B. Entanglement of qubit A_1 with $A_2 B$

Fig. 4 is a contour plot of global negativity $N_G^{A_1}(\rho_A^{II}(\tau))$ as a function of squeeze parameter s and interaction parameter τ , for initial state $|\Phi_2(0)\rangle$. As expected the interaction with squeezed field results in a decoherence of initial entanglement of qubit A_1 . Decoherence becomes more pronounced with increment in the value of parameter s . For $s \geq 0.5$, the peak value of $N_G^{A_1}$ is always less than one for the values of τ in the range shown in the plot. Fig. 5 displays $N_G^B(\rho_A^{II}(\tau))$ as a function of squeeze parameter s and interaction parameter τ , for initial state $|\Phi_2(0)\rangle$. While part of the initial state entanglement of qubit A_1 is transferred to field degrees a small part goes to increase the entanglement of remote qubit B with pair of qubits in cavity one. In this case the maximum value of negativity is 0.73, which corresponds to $s = 0.64$ and $\tau = 7.75$.

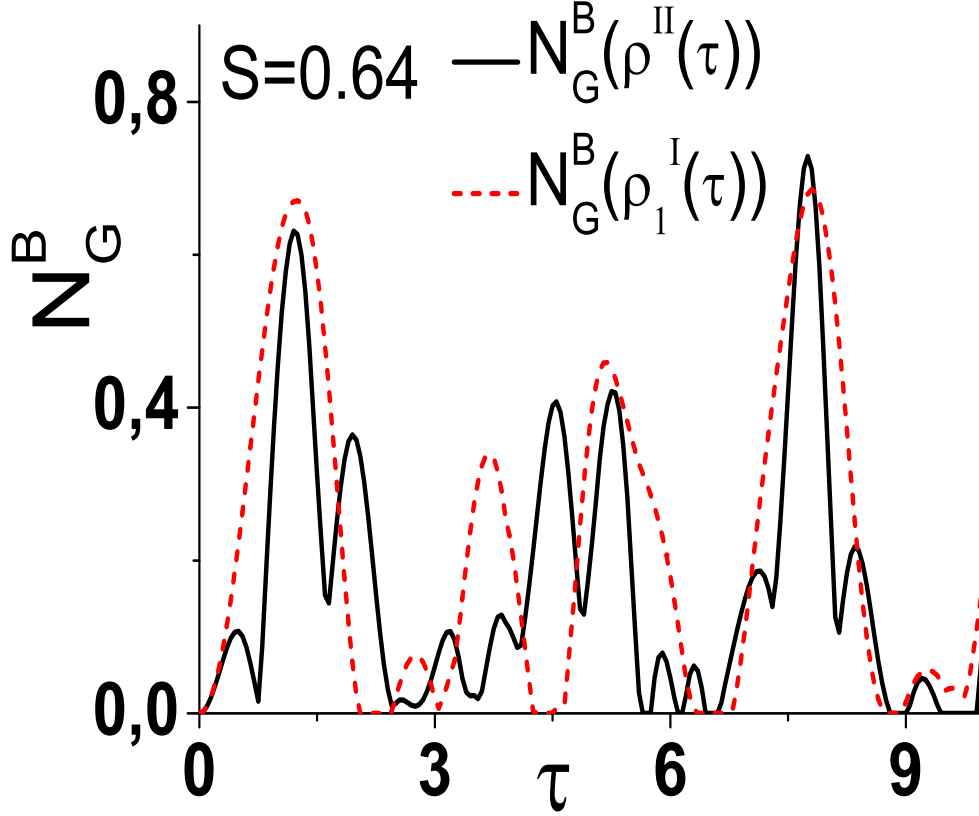


FIG. 6: N_G^B versus τ for $s = 0.64$, for initial states $|\Phi_2\rangle$ (solid line) and $|\Phi_1^{\alpha=1.0}\rangle$ (dashed line).

Figs. (6) and (7) display $N_G^B(\rho_A^{\alpha=1}(\tau))$ and $N_G^B(\rho_A^{II}(\tau))$ plotted for $s = 0.64$ and $s = 0.4$, respectively. It is seen that for initial state $|\Phi_2(0)\rangle$ the interaction time after which ESD occurs is longer than that for the case of separable initial state. The peak value of $N_G^B(\rho_A^{II}(\tau)) = 0.73$ is comparable to peak value of $N_G^B(\rho_A^{\alpha=1}(\tau)) = 0.7$ when $s = 0.64$. Figure 7 shows a decreased peak value of around 0.63 both for $N_G^B(\rho_A^{\alpha=1}(\tau))$ and $N_G^B(\rho_A^{II}(\tau))$. In the case of initial state $|\Phi_2(0)\rangle$, lowering the value of s increases the value of interaction parameter τ for which ESD occurs that is an increase in three qubit quantum correlations. The initially entangled state $|\Phi_2(0)\rangle$ with $s \leq 0.64$ is better suited to generate entanglement between the remote qubit B and the pair of qubits in cavity c_1 in comparison with initial states $|\Phi_1^\alpha(0)\rangle$.

IV. CONCLUSIONS

In this article, we have examined the entanglement generation due to interaction of an entangled pair of two level atoms A_1A_2 in cavity c_1 and an atom B in a remote cavity c_2 with two mode squeezed field shared by the cavities. Three qubit mixed state entanglement dynamics is a function of squeeze parameter value and initial state entanglement of the qubit pair A_1A_2 . Firstly, starting from different initial states, analytical expressions have been obtained for three qubit mixed state. The entanglement of qubits A_1A_2B is that of a W-like state, no genuine tripartite entanglement being generated. Numerical values of global negativity of partial transpose with respect to qubit B are used to search for initial states and squeeze parameter values that generate highly entangled states. We notice that the two mode squeezed field shared by two cavities generates entanglement of qubit B with pair of qubits A_1A_2 which reaches a peak value followed by sudden disappearance and revival. The dynamics of entanglement generation, sudden death and revival strongly depends on the three qubit initial state.

When both the atoms in cavity c_1 are prepared in ground state at $t = 0$, the entanglement of remote qubit is

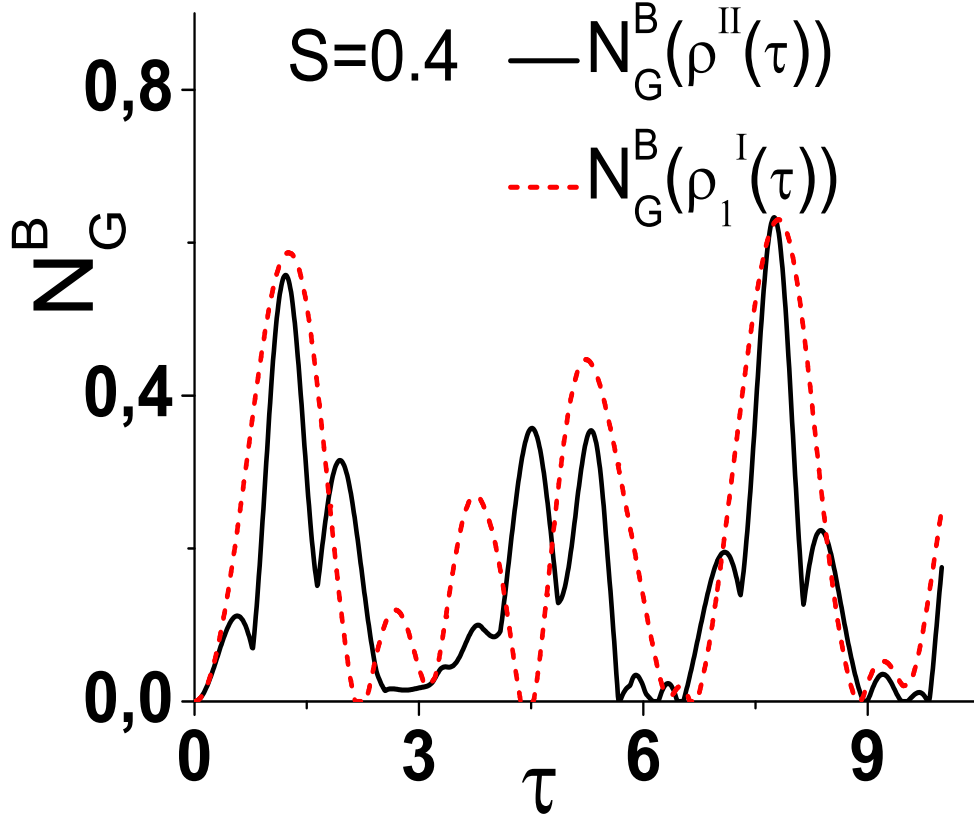


FIG. 7: N_G^B versus τ for $s = 0.4$, for initial states $|\Phi_2\rangle$ (solid line) and $|\Phi_1^{\alpha=1.0}\rangle$ (dashed line).

found to increase with s , being optimum for $s = 0.64$. This is significant from the point of view of practical utility of the mixed state entanglement. Starting with the pair of atoms A_1A_2 prepared initially in an entangled state $|\Phi_1^\alpha(0)\rangle = \sqrt{\alpha}|00\rangle + \sqrt{1-\alpha}|11\rangle$, the peak value of entanglement between the remote qubit B and pair of qubits A_1A_2 decreases as $\alpha \rightarrow 0$. With atoms A_1A_2 in state $|\Phi_2(0)\rangle = (|10\rangle + |01\rangle)/\sqrt{2}$ in first cavity, atom field interaction generates a three qubit mixed state with atom B in second cavity highly entangled to Bell pair A_1A_2 . In this case, entanglement transfer from the pair A_1A_2 partially compensates for the loss of entanglement due to state reduction. As a result, three qubit entanglement dynamics displays, relatively, longer sudden death free intervals. For a given value of squeeze parameter, the entanglement of remote qubit B with qubit pair A_1A_2 is of the same order as in the case when all three qubits are in a separable state, initially. However, a smaller value $s = 0.4$ under similar conditions generates a three qubit mixed state with comparable entanglement but lesser noise. We conclude that initially entangled state $|\Phi_2(0)\rangle$ with $s \leq 0.64$ is better suited to generate entanglement between the remote qubit B and the pair of qubits A_1A_2 in cavity c_1 in comparison with initial states $|\Phi_1^\alpha(0)\rangle$.

Financial support from, Capes Brazil, CNPq Brazil, Faep Uel Brazil, and Fundação Araucaria Pr Brazil is acknowledged.

-
- [1] A. K. Ekert, Phys. Rev. Lett. 67, 661 (1991).
 - [2] D. Bouwmeester, A. Ekert, and A. Zeilinger, The Physics of Quantum Information (Berlin: Springer) (2000).
 - [3] J. M. Raimond, M. Brune, and S. Haroche, Rev. Mod. Physics, 73, 565 (2001).
 - [4] Q. A. Turchette, C. S. Wood, B.E. King, C. J. Myatt, D. Leibfried, W. M. Itano, C. Monroe, and D. J. Wineland, Phys. Rev. Lett. 81, 3631 (1998).

- [5] H. Vahlbruch, M. Mehmet, S. Chelkowski, B. Hage, A. Franzen, N. Lastzka, S. Goßler, K. Danzmann, and R. Schnabel, *Phys. Rev. Letts.*, 100, 033602 (2008).
- [6] W. Son, M. S. Kim, J. Lee, and D. Ahn, *J. Mod. Opt.* 49, 1739 (2002).
- [7] M. Paternostro, W. Son, and M. S. Kim, *Phys. Rev. Lett.*, 92, 197901 (2004)].
- [8] P. J. dos Reis, and S. S. Sharma, *Phys. Rev. A* 79, 012326 (2009).
- [9] M. Paternostro, G. Adesso, and S. Campbell, *Phys. Rev. A* 80, 062318 (2009).
- [10] G. Adesso, S. Campbell, F. Illuminati, and M. Paternostro, *Phys. Rev. Lett.*, 104, 240501 (2010).
- [11] F. Casagrande, A. Lulli, and M. G. A. Paris, *Phys. Rev. A* 79, 022307 (2009).
- [12] B. Julsgaard, J. Sherson, J. I. Cirac, J. Fiursek, and E. S. Polzik, *Nature London* 432, 482 (2004).
- [13] M. D. Eisaman, A. Andr, F. Massou, M. Fleischhauer, A. S. Zibrov, and M. D. Lukin, *Nature London* 438, 837 (2005).
- [14] T. Chanelière, D. N. Matsukevich, S. D. Jenkins, S.-Y. Lan, T. A. B. Kennedy, and A. Kuzmich, *Nature London* 438, 833, (2005).
- [15] K. Zyczkowski, P. Horodecki, A. Sanpera, and M. Lewenstein, *Phys. Rev. A* 58, 883 (1998).
- [16] J. Eisert and M. Plenio, *J. Mod. Opt.* 46, 145 (1999).
- [17] G. Vidal and R. F. Werner, *Phys. Rev. A* 65, 032314 (2002).
- [18] W. Dür, G. Vidal, and J. I. Cirac, *Phys. Rev. A* 62, 062314 (2000).
- [19] S. S. Sharma and N. K. Sharma, *Phys. Rev. A* 76, 012326 (2007).
- [20] T. Yu and J. H. Eberly, *Phys. Rev.* 93,140404 (2004).
- [21] T. Yu and J. H. Eberly, *Opt. Commun.* 264, 393 (2006).
- [22] M. P. Almeida, F. de Melo, M. Hor-Meyll, A. Salles, S. P. Walborn, P. H. Souto Ribeiro and L. Davidovich, *Science* 316, 579 (2007).
- [23] Laurat, J., Choi, K. S., Deng, H., Chou, C. W., and Kimble, H. J., *Phys. Rev. Lett.* 99, 180504 (2007).
- [24] M. Tavis and F. W. Cummings, *Phys. Rev.* 170, 379 (1978).
- [25] A. Peres, *Phys. Rev. Lett.* 77, 1413 (1996).
- [26] M. Horodecki, P. Horodecki, and R. Horodecki, *Phys. Lett. A* 223, 1(1996).

Analytic expression for $\left| \Phi_{A_1 A_2 B}^{n-k, n-l}(\tau) \right\rangle_\alpha$ in Eq (17) reads as

$$\begin{aligned}
& \left| \Phi_{A_1 A_2 B}^{n-k, n-l}(\tau) \right\rangle_\alpha \\
&= \hat{U}_{12}^{n-k, n-l}(\tau) \left| \Phi_{A_1 A_2}^\alpha(0) \right\rangle |1, -1\rangle |n-k, n-l\rangle \\
&= \sqrt{\alpha} \cos(C_{nl}\tau) \frac{[B_{nk}^2 \cos(f_{nk}\tau) + A_{nk}^2]}{A_{nk}^2 + B_{nk}^2} |2, -2\rangle |1, -1\rangle |n-k, n-l\rangle \\
&\quad - i\sqrt{\alpha} (\cos C_{nl}\tau) B_{nk} \frac{\sin(f_{nk}\tau)}{\sqrt{(A_{nk}^2 + B_{nk}^2)}} |2, 0\rangle |1, -1\rangle |n-k-1, n-l\rangle \\
&\quad + \sqrt{\alpha} (\cos C_{nl}\tau) A_{nk} B_{nk} \frac{[\cos(f_{nk}\tau) - 1]}{A_{nk}^2 + B_{nk}^2} |2, 2\rangle |1, -1\rangle |n-k-2, n-l\rangle \\
&\quad - i\sqrt{\alpha} (\sin C_{nl}\tau) \frac{[B_{nk}^2 \cos(f_{nk}\tau) + A_{nk}^2]}{A_{nk}^2 + B_{nk}^2} |2, -2\rangle |1, 1\rangle |n-k, n-l-1\rangle \\
&\quad - \sqrt{\alpha} (\sin C_{nl}\tau) B_{nk}^2 \frac{\sin(f_{nk}\tau)}{\sqrt{(A_{nk}^2 + B_{nk}^2)}} |2, 0\rangle |1, 1\rangle |n-k-1, n-l-1\rangle \\
&\quad - i\sqrt{\alpha} (\sin C_{nl}\tau) A_{nk} B_{nk} \frac{[\cos(f_{nk}\tau) - 1]}{A_{nk}^2 + B_{nk}^2} |2, 2\rangle |1, 1\rangle |n-k-2, n-l-1\rangle \\
&\quad + \sqrt{1-\alpha} (\cos C_{nl}\tau) A_{n+2k} B_{n+2k} \frac{[\cos(f_{n+2k}\tau) - 1]}{A_{n+2k}^2 + B_{n+2k}^2} |2, -2\rangle |1, -1\rangle |n-k+2, n-l\rangle \\
&\quad - i\sqrt{(1-\alpha)} (\cos C_{nl}\tau) A_{n+2k} \frac{\sin(f_{n+2k}\tau)}{\sqrt{(A_{n+2k}^2 + B_{n+2k}^2)}} |2, 0\rangle |1, -1\rangle |n-k+1, n-l\rangle \\
&\quad + \sqrt{(1-\alpha)} (\cos C_{nl}\tau) \frac{[A_{n+2k}^2 \cos(f_{n+2k}\tau) + B_{n+2k}^2]}{A_{n+2k}^2 + B_{n+2k}^2} |2, 2\rangle |1, -1\rangle |n-k, n-l\rangle \\
&\quad - i\sqrt{(1-\alpha)} (\sin C_{nl}\tau) A_{n+2k} B_{n+2k} \frac{[\cos(f_{n+2k}\tau) - 1]}{A_{n+2k}^2 + B_{n+2k}^2} |2, -2\rangle |1, 1\rangle |n-k+2, n-l-1\rangle \\
&\quad - \sqrt{(1-\alpha)} (\sin C_{nl}\tau) A_{n+2k} \frac{\sin(f_{n+2k}\tau)}{\sqrt{(A_{n+2k}^2 + B_{n+2k}^2)}} |2, 0\rangle |1, 1\rangle |n-k+1, n-l-1\rangle \\
&\quad - i\sqrt{(1-\alpha)} (\sin C_{nl}\tau) \frac{[A_{n+2k}^2 \cos(f_{n+2k}\tau) + B_{n+2k}^2]}{A_{n+2k}^2 + B_{n+2k}^2} |2, 2\rangle |1, 1\rangle |n-k, n-l-1\rangle, \tag{25}
\end{aligned}$$

where

$$\begin{aligned}
A_{nk} &= \sqrt{(n-k-1)}, \quad B_{nk} = \sqrt{(n-k)}, \quad C_{nl} = \sqrt{(n-l)}, \\
A_{n+2k} &= \sqrt{(n-k+1)}, \quad B_{n+2k} = \sqrt{(n-k+2)}, \\
f_{nk} &= \sqrt{2(A_{nk}^2 + B_{nk}^2)}, \quad f_{n+2k} = \sqrt{2(A_{n+2k}^2 + B_{n+2k}^2)}. \tag{26}
\end{aligned}$$

The analytic form of $\left| \Phi_{A_1 A_2 B}^{n-k+1, n-l}(\tau) \right\rangle$ in Eq. (20) is given by

$$\begin{aligned}
& \left| \Phi_{A_1 A_2 B}^{n-k+1, n-l}(\tau) \right\rangle \\
= & -i \cos(C_{nl}\tau) B_{n+1k} \frac{\sin(f_{n+1k}\tau)}{\sqrt{(A_{n+1k}^2 + B_{n+1k}^2)}} |2, -2\rangle |1, -1\rangle |n-k+1, n-l\rangle \\
& + \cos(C_{nl}\tau) \cos(f_{n+1k}\tau) |2, 0\rangle |1, -1\rangle |n-k, n-l\rangle \\
& -i \cos(C_{nl}\tau) A_{n+1k} \frac{\sin(f_{n+1k}\tau)}{\sqrt{(A_{n+1k}^2 + B_{n+1k}^2)}} |2, 2\rangle |1, -1\rangle |n-k-1, n-l\rangle \\
& - \sin(C_{nl}\tau) B_{n+1k} \frac{\sin(f_{n+1k}\tau)}{\sqrt{(A_{n+1k}^2 + B_{n+1k}^2)}} |2, -2\rangle |1, 1\rangle |n-k+1, n-l-1\rangle \\
& -i \sin(C_{nl}\tau) \cos(f_{n+1k}\tau) |2, 0\rangle |1, 1\rangle |n-k, n-l-1\rangle \\
& - \sin(C_{nl}\tau) A_{n+1k} \frac{\sin(f_{n+1k}\tau)}{\sqrt{(A_{n+1k}^2 + B_{n+1k}^2)}} |2, 2\rangle |1, 1\rangle |n-k-1, n-l-1\rangle.
\end{aligned} \tag{27}$$